Journal of Sound and Vibration (1998) **217**(1), 145–161
Article No. sv981760

A VIBRATION MODEL OF OPEN CELLED POLYURETHANE FOAM AUTOMOTIVE SEAT CUSHIONS

W. N. Patten, S. Sha and C. Mo

Automotive Ride Engineering Laboratory, *The University of Oklahoma*,
865 *Asp Avenue*, *Room* 212, *Norman*, *OK* 73019, *U.S.A.*
Email: wpatten@ou.edu

(*Received* 21 *February* 1997, *and in final form* 20 *May* 1998)

A mechanistic model of a seat cushion is developed. The work relates the kinematic motion of the seat to the geometric and constitutive properties of the cellular foam used in the seat. The model includes the influence of pneumatic damping caused by friction between the gas within the open-celled foam and matrix polymer. A continuous shape function is introduced to characterize the piecewise continuous stress–strain characteristic of flexible open-celled foam. After some simplification, a non-linear dynamic automotive seat cushion model is derived, which relies explicitly on the constitutive properties of polyurethane foams and on the geometry of the seat cushion. Experimental and analytical models of the two automotive seats are compared to verify the model. The comparisons indicate that the new model is able to predict the dynamic performance of an automotive seat cushion with fidelity.

1. INTRODUCTION

Open cell polyurethane (PUR) foam has become the preferred material for automotive seat cushion construction. It provides a significant decrease in the weight/performance ratio when compared to more traditional steel spring seat support systems. The most attractive feature of the material is that it makes it possible to construct a seat at a cost that is much reduced from the cost realized when using more traditional materials. The design of a seat can affect both static (posture) and dynamic (vibration) comfort. Seat design has been conducted in the past without the benefit of a clear understanding of the dynamic characteristic of the foam used in automotive seat cushions. This paper describes the development of a low order mechanistic model of a seat cushion in which the dependence of the model parameters on the constitutive properties of PUR is established. Open cell PUR foam consists of a polymer matrix and an entrained fluid or gas. The gas is able to flow though the polymer matrix under the action of an imposed load. The movement of the gas through the matrix can affect the mechanical properties of the foam. The stiffness of the polymer matrix is also a significant source of variation of the physical properties of PUR. The stiffness characteristics of PUR are inherently related to the level of loading. Low loads are dominated by simple,

0022–460X/98/410145 + 17 $30.00/0

linear elastic bending. Loads beyond the linear-elastic range produce elastic buckling of the PUR foam. Loads far beyond the buckling range culminate in a significant effect. These various mechanisms provided the basis for the modelling proposed herein.

2. BACKGROUND

Models that are routinely used to predict the behavior of cellular materials are often based on phenomenological behavior [1, 2] to explain the influence of closed cell structures on the compressive stress–strain behavior of a semi-rigid foam. The broad field of modelling of foams has previously been reviewed [3]. One of the most widely employed modelling approaches [4] proposed the use of a square-section structural strut in the study of the elastic properties of the stress–strain behavior of open cell flexible foams. The authors assumed that the cubes of material at the junctions of the struts are undeformable. While their analysis was performed in the context of latex rubber foams which have an irregular cell structure, the structural model is general enough to apply to most open cell polymer foams. A theory was developed for the dynamic mechanical behavior of open cell flexible foams containing compressible and incompressible fluids, but the resulting equations were applicable to small strains only [5, 6].

A report on the time and temperature dependence of high density foams used in automotive seats [7], indicated that apparent relaxation times may be determined from compression set versus time test curves. These values make possible the determination of other useful properties of the foam, including the viscosity at any practical temperature, the glass transition temperature and the energy of activation for fluidization of the foam. Investigators [8] discussed the structure of cellular solids, their properties, and engineering design methods for cellular foams. They include an extensive treatment of the stress–strain behavior of foams. A comprehensive review of the mechanics and elasto-dynamics of open-celled foams [9] suggests that lumped parameter models of non-linear mechanisms might be adequate to define the time–stress–strain relations for a block of cellular foam.

Automotive seats were for generations constructed with steel springs and layers of material to distribute the local forces at the posterior of the rider. Cellular foam materials were adopted for seat construction in the 60s because of their reduced cost, high degree of manufacturability and because they provide a reasonable amount of ride comfort. A good seat has been defined as one that (1) gives good support to the drive and passengers in every driving situation, (2) reduces the transmission of vibration from the car to the body of the passenger, and (3) provides a comfortable seat with respect to temperature and humidity [10] It is noted that the molded flexible polyurethane seat fulfills all these requirements. The mechanics and design of polymer cushioning, in terms of comfort, examined the effect force–deflection behavior, material hysteresis, sag factor, breath ability and resilience played in making an assessment of seat foam comfort [11].

3. MODELLING

The work here assumes that motions relative to static equilibrium are small. While a linear model would seem reasonable, it is reported that nonlinear effects may be important (even at small vibration amplitudes) to a study of vibration seat comfort [12]. A seat cushion model is suggested here that includes non-linear elastic compliance and damping effects.

Open cell foams exhibit a repetitive three dimensional geometric structure (Figure 1). Different geometric shapes and cell edge size give foams their different properties. Cell size can vary from a narrow to a broad aspect ratio. A seat cushion/suspension system is treated as a two degree-of-freedom (DOF) dynamic system incorporating a lumped mass, the cushion and a linear elastic suspension (Figure 2). The cushion is assumed to be constructed of PUR open cell foam with air entrapped in the cell matrix. The cushion suspension spring is generally much stiffer than the foam.

It is assumed that the local stress in the material matrix can be represented as the superposition of elastic stress and stress effect due to flow of the entrapped gas [9]:

$$\sigma = \sigma_e + \sigma_f. \tag{1}$$

The major assumptions of the model are: (1) the foam consists of an assemblidge of cells; (2) the top and sides of the foam cushion are covered with a material that prevents flow though those faces of the cushion; (3) the motion is assumed to occur in the vertical direction only; (4) the air in the foam matrix is treated as a Newtonian fluid; and (5) flow is assumed incompressible, which is justified for low Reynolds numbers.

Figure 3 depicts a typical stress–strain curve for an open celled PUR. Three phases are evident. First, the foam acts much like any linear elastic material over

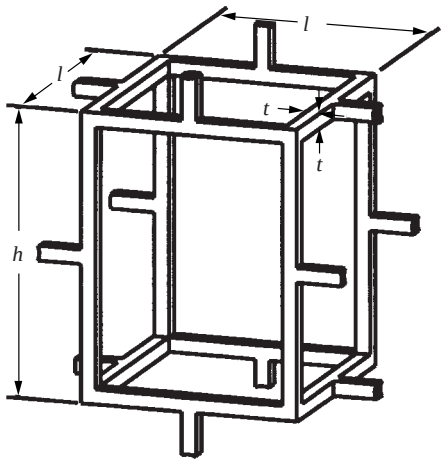

Figure 1. A square prism mold for open cell foam (reprinted from reference [8]).

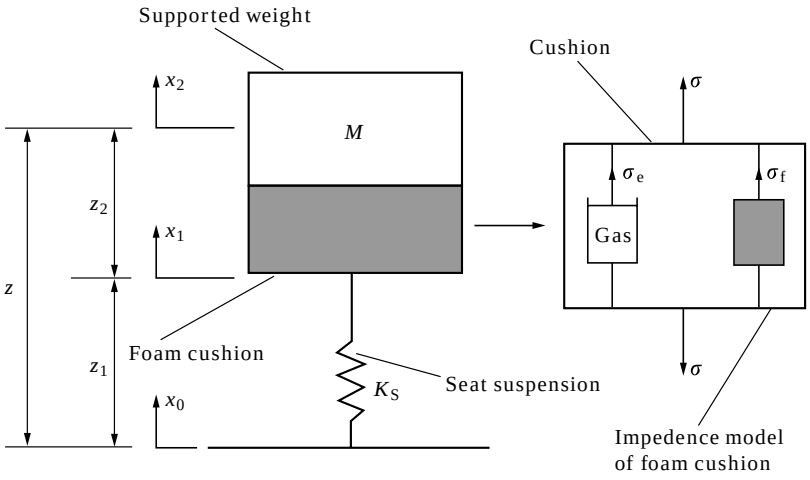

Figure 2. Two-DOF model of seat.

a short range of strains ($\varepsilon < 0{\cdot}05$) [8]. In this phase the walls of the open celled foam provide simple bending resistance to loads. In the second phase, the walls of the cellular structure suffer progressive buckling. This phase is typified by a softening or reduction of the stiffness of the foam structure. The last phase of the stress–strain characteristic shown in Figure 3 represents the densification stage. Buckling is complete in this last phase and the entrained gas has been expelled or is physically trapped in the crushed matrix. This last phase is evidenced by a steeply increasing stiffness. The work here assumes that the seat cushion dynamics occur within phase one and two of the stress–strain characteristic.

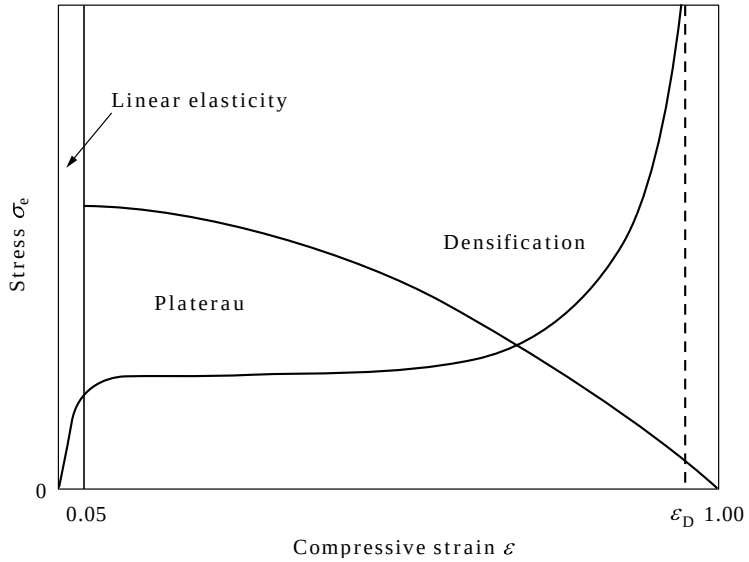

Figure 3. Stress–strain curve for open cell foam.

Previous investigators [8] proposed the following piecewise smooth model for the stress–strain characteristic of a PUR open celled foam:

$$\sigma_m = \begin{cases} E_S\left(\dfrac{\rho^*}{\rho_S}\right)^2 \varepsilon, & \varepsilon \leqslant 0{\cdot}05, \\ 0{\cdot}05E_S\left(\dfrac{\rho^*}{\rho_S}\right)^2, & 0{\cdot}05 < \varepsilon \leqslant \varepsilon_D\left(1 - \dfrac{1}{D}\right), \\ \dfrac{0{\cdot}05}{D} E_S\left(\dfrac{\rho^*}{\rho_S}\right)^2 \left(\dfrac{\varepsilon_D}{\varepsilon_D - \varepsilon}\right)^m, & \varepsilon > \varepsilon_D\left(1 - \dfrac{1}{D}\right). \end{cases} \tag{2}$$

The work here relies on the development of a smooth shape function that approximates the stress–strain behavior defined by equation (2):

$$\sigma_m = E_f \varepsilon F(\varepsilon), \tag{3}$$

where E_f is the initial Young's modules. The form of $F(\varepsilon)$ proposed here is

$$F(\varepsilon) = a(c + d_1\varepsilon)^{-p_1} + b\varepsilon^q. \tag{4}$$

where a, b, c, d_1, p_1 and q are positive constants. This expression (4) differs from Gent and Rusch [9], in that an offset (c) is added in order to provide a better fit to the data. The stress is then

$$\sigma_e = E_f[a(c + d_1\varepsilon)^{-p_1} + b\varepsilon^q]\varepsilon. \tag{5}$$

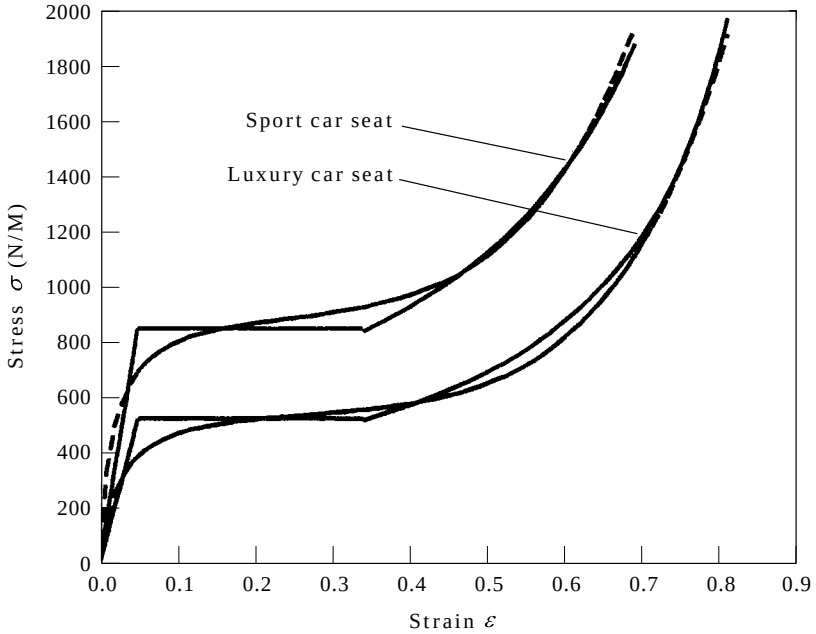

Figure 4. Comparison of quasi-static stress–strain behavior: ——, theoretical; – – –, stress expressed by shaped function.

Figure 4 is a comparison of equations (2) and (5) for two kinds of automotive seats. The parameters used in equation (4) are given in Table 1.

Because strain is <1, then the magnitude of the parameter q indicates that the term $b\varepsilon^q$ can be neglected. The stress–strain relationship then takes the hyperbolic form

$$\sigma_m = E_f \frac{a}{(c + d_1\varepsilon)^{p_1}} \varepsilon. \tag{6}$$

The work here assumes that the dissipation of energy in open celled foams under dynamic loads is due to fluid flow loss. The model proposed here is consistent with previous studies [5, 6, 9, 13]. Those investigators proposed shock absorption models of open celled foams that relied on fluidic losses to account for observed damping effects. When a dynamic load is applied to the foam, the pressure of the entrained gas increases which results in a flow potential. The cushion is modelled as a rectangular block of open cell foam of cross sectional area A, and height H. When loaded, the foam matrix deforms in the Z direction. The gas contained in the cells is forced to flow out the bottom surface of the cushion. The velocity which is assumed to vary uniformly in the Z direction, and the flow is opposed by a differential pressure.

TABLE 1

Seat parameters

Volume fraction of open cell matrix§ Parameter title	Symbol Symbol	Ns/m^2 Unit	$1{\cdot}85 \times 10^{-5}$ Luxury car	$1{\cdot}85 \times 10^{-5}$ Sport car
Foam cell edge thickness†	t	m	6×10^{-5}	6×10^{-5}
Foam cell edge length†	l	m	9×10^{-4}	8×10^{-4}
Foam cell diameter†	d	m	9×10^{-4}	8×10^{-4}
Cushion height†	H	m	$6{\cdot}7 \times 10^{-2}$	4×10^{-2}
Cushion area†	A	m^2	$9{\cdot}5 \times 10^{-2}$	9×10^{-2}
Mass of sandbag†	M	kg	36	36
Young's module of polymer‡	E_s	N/m^2	6×10^7	6×10^7
Young's module of foam	E_f	N/m^2	$1{\cdot}1 \times 10^4$	$1{\cdot}7 \times 10^4$
Density of air‡	ρ	kg/m^3	1·22	1·22
Viscosity of air‡	μ	Ns/m^2	$1{\cdot}85 \times 10^{-5}$	$1{\cdot}85 \times 10^{-5}$
Relative density of foam§	ρ^*/ρ_s		0·0133	0·0169
Volume fraction of open cell matrix§	ζ		0·0133	0·0169
Surface factor†	K_b		1	0·4
Coefficients of shape function¶	a		5×10^{-4}	$1{\cdot}05 \times 10^{-3}$
	b		0·4	0·4
	c		$2{\cdot}2 \times 10^{-4}$	$3{\cdot}4 \times 10^{-4}$
	d_1		0·009	0·0189
	p_1		1	1
	q		4·5	4·5

† Measured data.
‡ Handbook reference data.
§ Calculated data.
¶ Data fit.

Flow is governed by the energy balance

$$\frac{\mathrm{d}p}{\rho g} + \frac{d(\bar{V}^2)}{2g} = -d(W_\mathrm{f}) - d(W_\mathrm{k}), \tag{7}$$

where $\bar{V}$ is the relative average velocity between gas flow and matrix polymer, ρ is density of the gas, W_f represents viscous fluid loss and W_k is the kinetic energy loss due to turbulence. If the flow is viscous, and if inertia effects are neglected then it can be shown that Darcey's equation holds:

$$\Delta p = -\frac{\mu}{K}\bar{V}\,\mathrm{d}Z, \qquad K = \frac{d^2}{32}. \tag{8}$$

The energy loss caused by friction, W_f is then

$$W_\mathrm{f} = -\frac{1}{\rho g}\frac{\mu}{K}\bar{V}\,\mathrm{d}Z. \tag{9}$$

It has been suggested [5, 6] that the kinetic loss due to turbulence is

$$W_\mathrm{k} = \frac{\Delta p}{\rho g} = -\frac{1}{\rho g}\bar{V}^2\,\mathrm{d}Z. \tag{10}$$

It has been found that both K and B (defined below) are independent of the fluid, whether it be compressible or incompressible, and that for a range of open cell foams $K \cong 0{\cdot}012d^2$ [9]. The coefficient B is defined as

$$B = \frac{(D^2-1)^2}{2d}, \tag{11}$$

where D is the ratio of the diameter of the nominal flow path to the diameter of the nominal constriction. Defining

$$\zeta = \frac{\rho^*}{\rho}, \qquad \bar{v} = \frac{(H-Z)}{\zeta}\cdot\dot{e}, \tag{12}$$

and substituting equations (9) and (10) into equation (7) yields

$$\frac{\mathrm{d}p_\mathrm{g}}{\mathrm{d}Z} = \frac{\mu(H-Z)}{K\zeta}\dot{\varepsilon} + \frac{\rho}{K_\mathrm{b}^2\zeta^2}\left[(H-Z) + \frac{1}{B}(H-Z)^2\right]\dot{\varepsilon}^2, \tag{13}$$

where $\dot{\varepsilon}$ is strain rate. K_b is fraction of the total potential open flow area. Because B is very small [8], the last term in equation (13) can be disregarded. Integrating equation (14) (let $p(0) = 0$) yields

$$p_\mathrm{g} = \left[\frac{\mu}{2K\zeta}\dot{\varepsilon} + \frac{\rho}{2K_\mathrm{b}^2\zeta^2}\dot{\varepsilon}^2\right](2H-Z)Z, \tag{14}$$

integrating over the depth of the cushion and dividing by the height produces an average stress–strain relationship for the cushion,

$$\sigma_\mathrm{f} = \frac{\mu H^2}{3K\zeta}\dot{\varepsilon} + \frac{\rho H^2}{3K_\mathrm{b}\zeta^2}\dot{\varepsilon}^2. \tag{15}$$

The first term on the right-hand side of equation (15) represents linear viscous loss. The second term represents turbulent flow resistance. The importance of the term is of course questionable when one realizes that strains and strain rates are necessarily small when treating auotomotive seat vibration. When substituting equations (6) and (15) into equation (1), the total stress in the foam cushion then becomes

$$\sigma = E_f \frac{a}{(c + d_1\varepsilon)^{p_1}} \varepsilon + \frac{\mu H^2}{3K\zeta} \dot{\varepsilon} + \frac{\rho H^2}{3K_b^2\zeta^2} \dot{\varepsilon}^2. \tag{16}$$

Applying Newton's second law to the seat cushion, the equation of motion for the system is

$$M\ddot{Z} = -E_f \frac{aA}{(cH + d_1|Z|)^{p_1}} Z - \frac{\mu AH}{3K\zeta} \dot{Z} - \frac{\rho A}{3K_b\zeta^2} |\dot{Z}|\dot{Z} - M\ddot{X}_0. \tag{17}$$

4. MODEL VALIDATION

A test station was constructed that consisted of an electrohydraulic motion simulator, a PC-based control system and a data acquisition system. The setup also included a signal conditioning system and a real time wave form dynamic analyzer (Figure 5). The seat motion simulator has the capacity to replicate the time trace of the recorded floor/seat track motion of a vehicle with high fidelity. The feedback control performance of the seat simulator is characterized by both a flat amplitude and a flat phase response over the entire bandwidth of frequencies (0–30 Hz) where humans are sensitive to vibration [14]. The simulator has a test bandwidth of 35 Hz. Piezoresistive accelerometers were used that have a flat

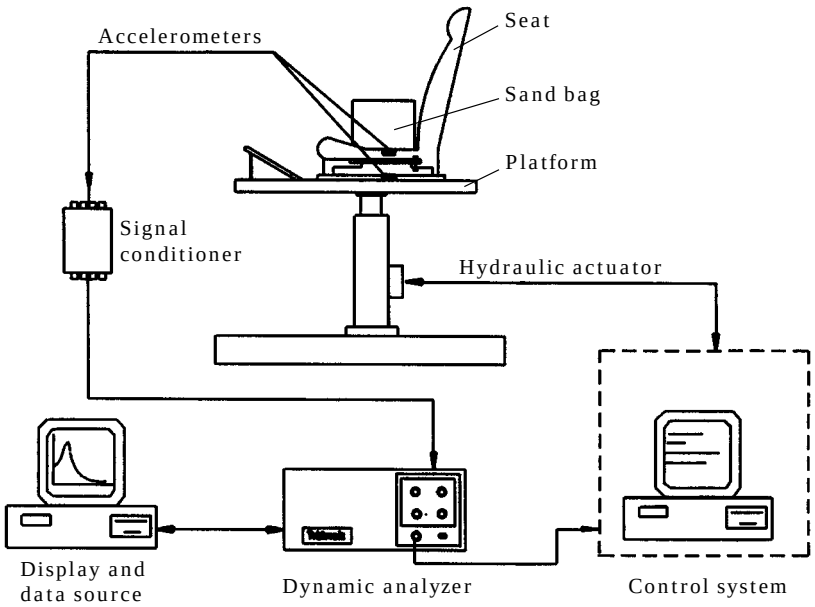

Figure 5. Experimental setup.

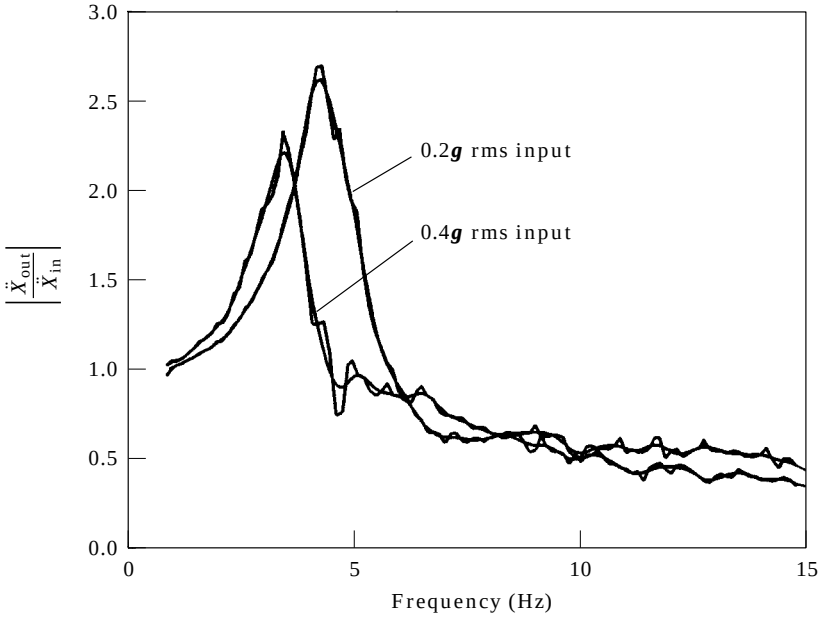

Figure 6. Experimental transfer function of a luxury car seat for 356 N (80 lb) seat load (raw data and smoothed data shown).

response from DC to 1 kHz. Accelerometers were placed at the seat butt and at the seat track to measure vertical acceleration. The bandwidth of the signal condition amplifier was 6 kHz. The data was collected at 500 Hz. Post analysis of the data was accomplished using MATLAB. All response spectrums were verified during testing by using a dynamic analyzer.

The driver's seat from two different vehicles, a luxury car and a sport car, were used in the tests. Each seat was mounted one at a time for testing on the simulator. A tightly packed plastic bag, containing sand and weighing 356 N (80 lb), was placed on the seat cushion. The platform and seat track were vibrated vertically with a random noise acceleration. The acceleration input level used ranged from 0·05 $\boldsymbol{g}$ rms to 0·45 $\boldsymbol{g}$ rms, in increments of 0·05 $\boldsymbol{g}$ rms. An analyzer was used to compute the transfer function of the seat butt vertical acceleration to the seat track vertical acceleration. The amplitude of the input was then increased by 0·05 $\boldsymbol{g}$ and the process repeated. Figures 6 and 7 provide comparisons of transfer functions of a luxury car seat and a sport car seat using a 0·2 $\boldsymbol{g}$ rms and 0·4 $\boldsymbol{g}$ rms inputs. Figures 8 and 9 depict all of the experimentally measured transfer functions for the two seats. The experimental results (Figures 6–9) indicate that automotive seats behave non-linearily. Both the peak amplitude and the resonant frequency decrease with increasing seat track acceleration input. If the seat cushion compliance was linear, then the transfer function would be identical for any input amplitude. The experimental results also provide a clue as to why the luxury car seat is generally perceived [15] to be more comfortable than the sports car seat. Peak amplitudes of each transmissibility curve for the luxury car seat occur below 5 Hz. Noting that seated humans are particularly sensitive to vertical vibration at about 6 Hz (spinal resonance) [16], it is clear that the luxury car seat attenuates

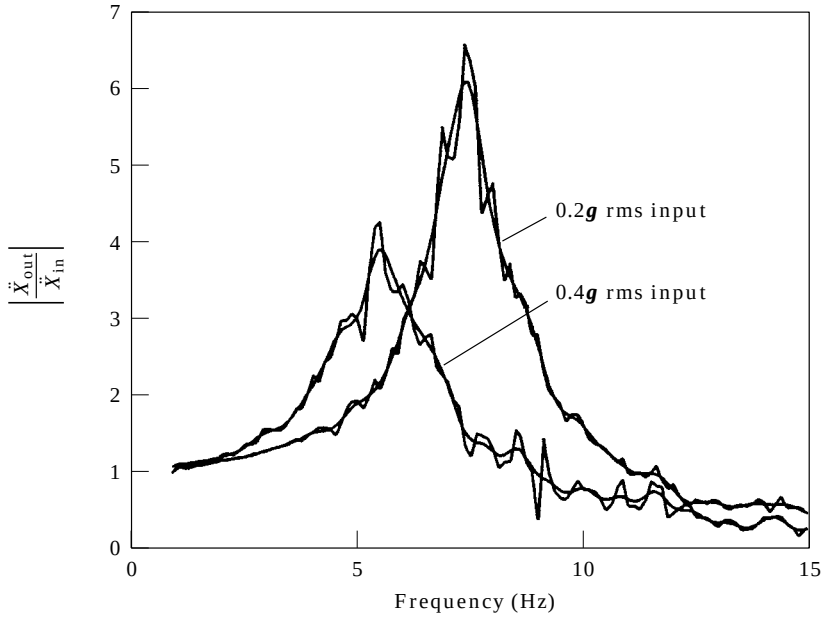

Figure 7. Experimental transfer function of a sport car seat for 356 N (80 lb) seat load (raw data and smoothed data shown).

all inputs at that frequency. The sports car seat on the other hand, amplifies inputs at the spinal resonance. The nature of the change in response that occurs with increased passenger weight is indicated in Figures 10 and 11. The results clearly indicate that cushion response is also sensitive to the weight of the supported load.

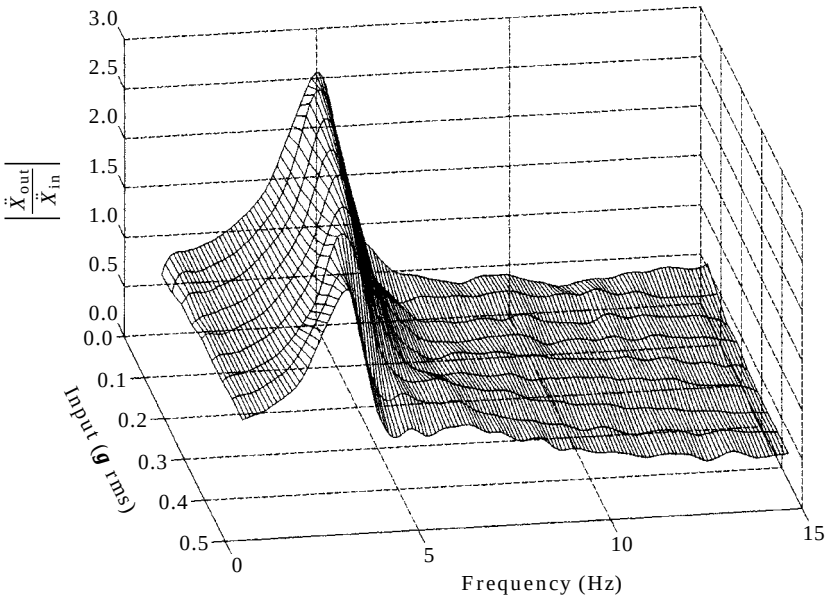

Figure 8. Measured transfer function of a luxury car seat for 356 N (80 lb) seat load (smoothed).

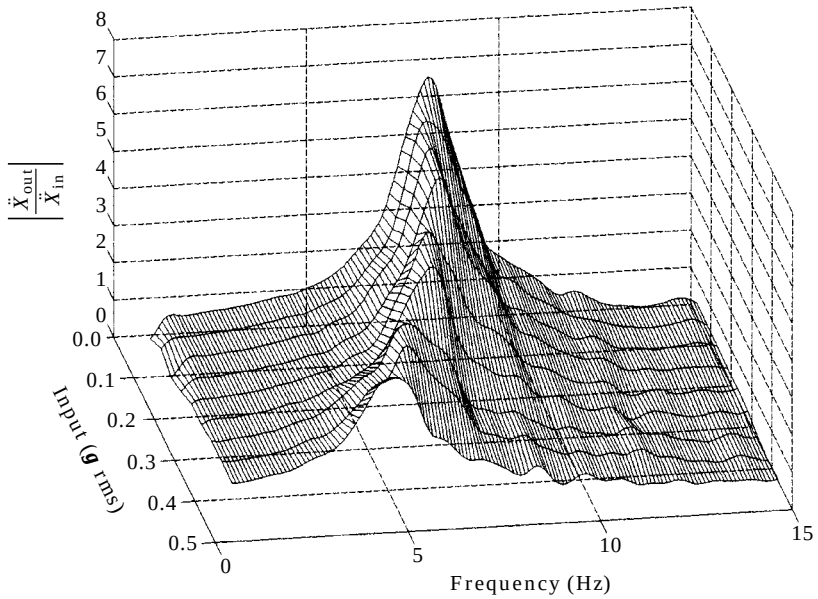

Figure 9. Measured transfer function of a sport car seat for 356 N (80 lb) seat load (smoothed).

The experimental data was used to determine the accuracy with which the proposed model could mimic the measured response. A set of nominal parameters was adopted based on measurements of the foam in each seat cushion (Table 1). Next, shape function coefficients were determined (Table 2). Simulations were then conducted. A white noise acceleration was assumed as the seat track input and

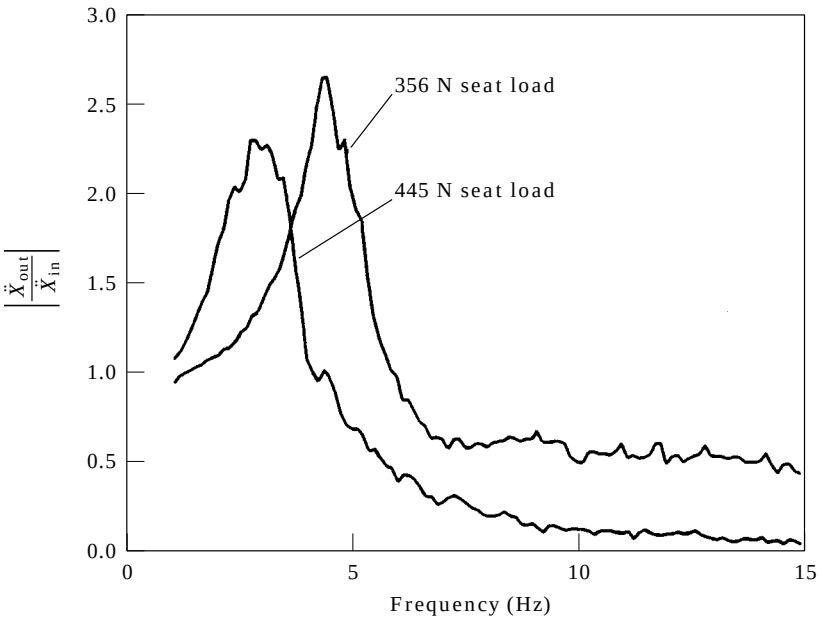

Figure 10. Comparison of experimental transfer function of a luxury car seat for different seat load with 0·2 ***g*** rms input.

TABLE 2

Shape function parameters†

Parameters	Luxury car seat		Sport car seat	
	With spring	Without spring	With spring	Without spring
a	0·0005	0·0005	0·00105	0·00105
b	0·3	0·4	0·2	0·4
c	0·00022	0·00022	0·00034	0·00034
d_1	0·009	0·009	0·0189	0·0189
p_1	1	1	1	1
q	8	4·5	8·5	4·5

† Parameters were selected to provide best fit to standard quasi static characteristic.

the response of the seat/mass system was simulated. The response was obtained by numerical integration. The simulated transfer functions were obtained using standard FFT software. A transfer function was generated for a sequence of seat track acceleration inputs ranging from 0·05 ***g*** rms to 0·45 ***g*** rms. The collection of simulated transfer functions for both seats with a 356 N (80 lb) seat load are presented in Figures 12 and 13. A comparison of Figures 8 and 9 with Figures 12 and 13 indicates a close correspondence of the model versus the actual (measured) response. Figure 14 depicts the simulated and experimental transfer functions of both car seats for a 0·2 ***g*** rms vertical white noise excitation inputs. Next, the model was used to simulate the response of the two seats for an increased seat load;

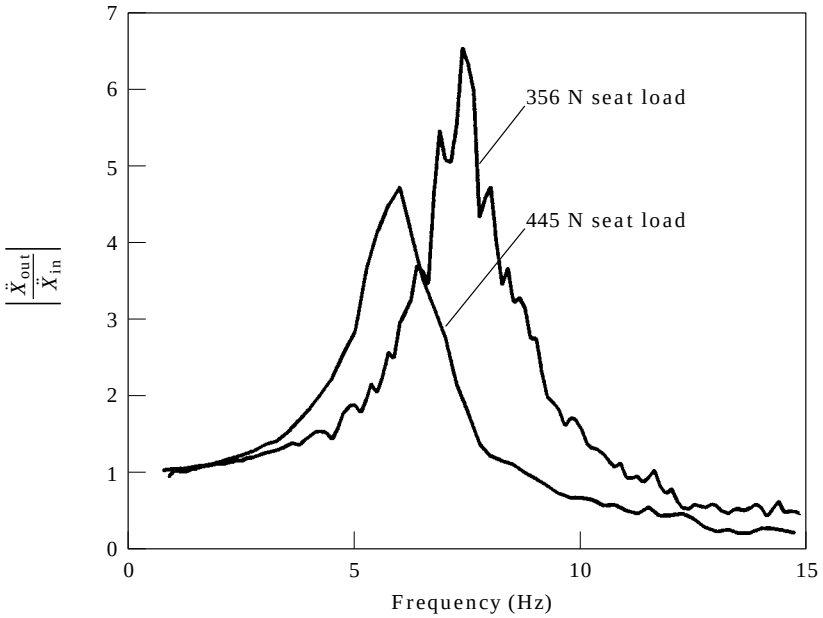

Figure 11. Comparison of experimental transfer function of a sport car seat for different seat load with 0·2 ***g*** rms input.

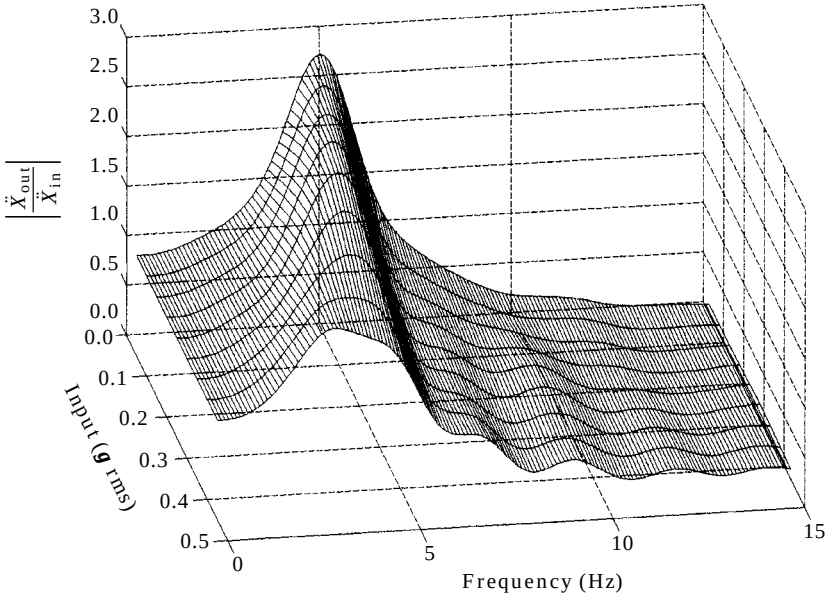

Figure 12. Smoothed simulated transfer function of a luxury car seat for 356 N (80 lb) seat load.

Figure 15. The results suggests that the coefficients in the proposed model are insensitive to pay load variations, for the range of inputs tested.

Finally an inventory of the contribution of each of the three force terms in equation (16) was conducted (Figure 3). In the case of the luxury car the percentage contribution of the quadratic damping force never exceeds 1%. The open question then was whether damping played any significant role in the test

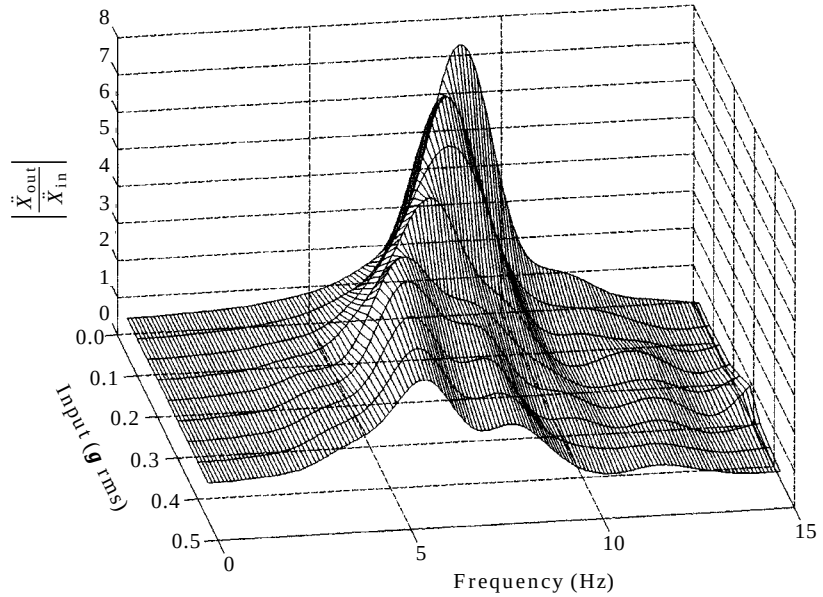

Figure 13. Smoothed simulated transfer function of a sport car seat for 356 N (80 lb) seat load.

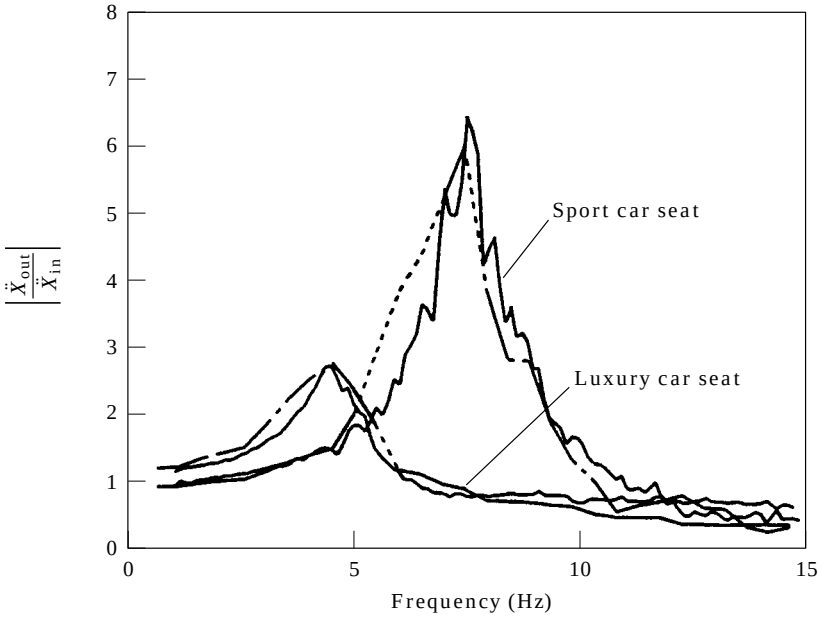

Figure 14. Comparison of raw experimental versus simulated transfer functions of luxury car seat and sport car seat with 356 N (80 lb) seat load for 0·2 ***g*** rms input: ——, raw data; – – – –, smoothed data.

results. It had already been established that without the inclusion of damping, the model was unable to mimic the measured response. A heuristic approach was used to establish the importance of damping. Each seat model was subjected to a

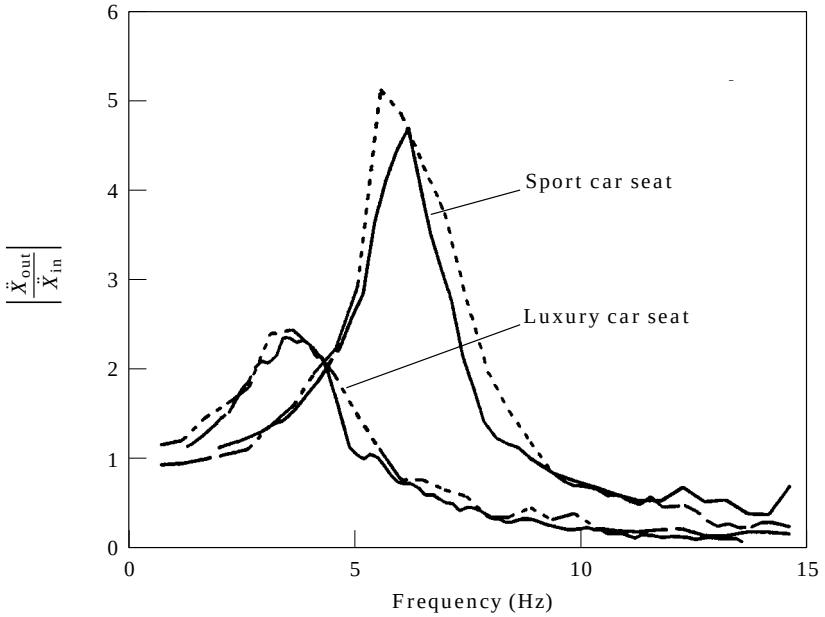

Figure 15. Comparison of raw experimental versus simulated transfer functions of luxury car seat and sport car seat with 445 N (100 lb) seat load for 0·2 ***g*** rms input: ——, raw data; – – – –, smoothed data.

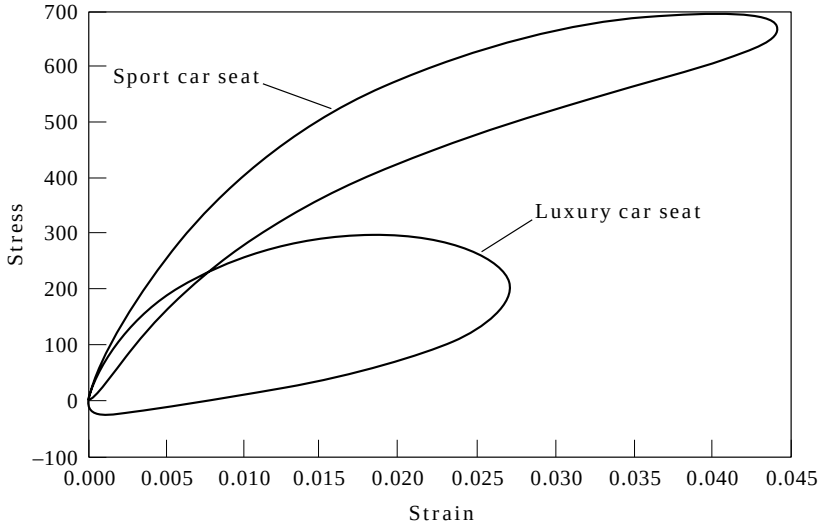

Figure 16. Steady state response of seat track and 356 N (80 lb) sand bag to a sinusoidal acceleration $\ddot{x} = 0{\cdot}2\,\boldsymbol{g}\,\sin(2\pi \cdot 5t)$.

sinusoidal seat track input at 5 Hz. The magnitude of the seat track acceleration was varied over the range from 0·05 $\boldsymbol{g}$ rms to 0·45 $\boldsymbol{g}$ rms. A plot of the force (input) versus strain was recorded. Figure 16 depicts the response for both the luxury and sports car seat for a 5 Hz input at 0·2 $\boldsymbol{g}$ rms. The area enclosed by each diagram was tabulated. That area, which represents the work (energy) dissipated per cycle, was then recorded for each of the test inputs between 0·05 $\boldsymbol{g}$ and 0·45 $\boldsymbol{g}$. Figure 17 depicts the results for the entire test range of seat track inputs. Two things are immediately obvious. First there is very little difference in the absorbed energy for

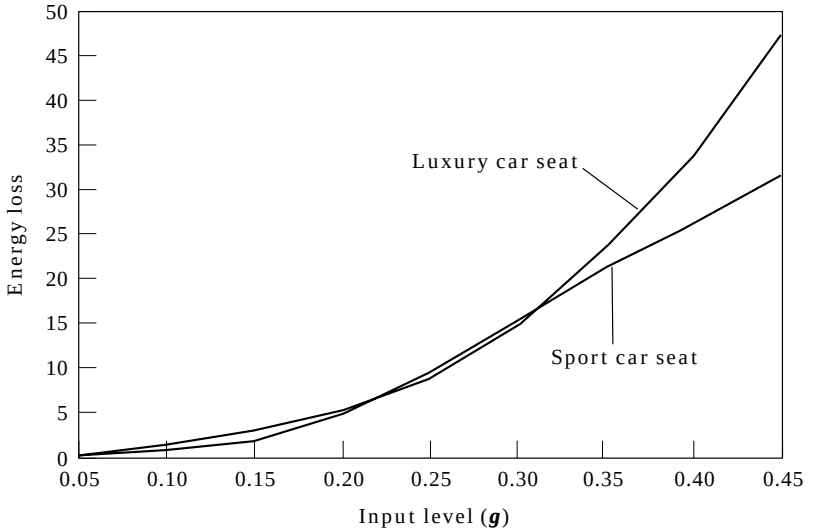

Figure 17. Energy dissipated per cycle of seat cushion using 5 Hz seat track acceleration input with different peak values. An 356 N (80 lb) sand bag was mounted on seat cushion.

both seats through $0{\cdot}35\,\boldsymbol{g}$. At very large acceleration inputs the luxury car hysteresis increase dramatically. Perhaps, the most important observation is that the damping ratio for both seats at all $\boldsymbol{g}$ levels $<0{\cdot}35\,\boldsymbol{g}$ is essentially a constant, and that constant is almost the same for both seats. The data suggests that the essence of each seat's dynamic response characteristic is defined almost entirely by the stiffness of the open celled foam used in the seat cushion. The data indicates that the dominate model feature of an open celled polyurethene seat is the nonlinear elastic stiffness. This is in sharp contrast to previous work which indicated that damping is the critical feature of the design of a seat [17].

5. CONCLUSIONS AND RECOMMENDATIONS

A non-linear vibration model of automotive seat cushions was presented. The model was derived using fundamental laws of mechanics and hydraulics. It includes non-linear stiffness and, linear and non-linear fluid damping effects. The non-linear stiffness was shown to be characteristic of the mechanical properties of the open-celled foam that is used in the construction of an automobile seat cushion. Those elastic response characteristics include the progressive load phases of bending and bucking. The model assumes that the deformation associated with normal ride vibrations is not sufficient to cause compaction of the cell structure. Damping was characterized as a friction loss realized as the entrained gas in the foam matrix flows under load. The significant contribution reported in this paper was *the development of a low order model of an automotive seat that is characterized by parameters that are directly related to the physical characteristics of the open-celled foam used to construct the seat*.

The model was shown to provide a good fit to the measured data for all input levels. The model was also shown to provide an excellent prediction of the response for different seat occupant weights. The model provides a new tool for the chassis, suspension and seat engineers that are charged with the design and analysis of seats and seat vibration isolation systems.

REFERENCES

1. R. E. Skochdopole and C. C. Rubens 1965 *Journal of Cellular Plastics* **1**, 91–103. Physical property modifications of low density polyethylene foams.
2. D. R. Moore, K. H. Couzens and M. J. Iremonger 1974 *Journal of Cellular Plastics* **10**, 135–141. The deformational behavior of foamed thermoplastics.
3. E. A. Meinecke and R. C. Clark 1973 *Mechanical Properties of Polymeric Foams*. Westport, Conn: Technomic.
4. A. N. Gent and A. G. Thomas 1963 *Rubber Chemistry Technology* **36**, 597–615. Mechanics of foamed elastic materials.
5. A. N. Gent and K. C. Rusch 1966 *Rubber Chemistry Technology* **39**, 389–402. Viscoelastic behavior of open cell foams.
6. K. C. Rusch 1966 *Ph.D. Thesis*, *University of Akron*, *Ohio*. Viscoelastic behavior of open cell foams.
7. S. M. Terry 1975 *Cellular Plastics in Transportation*, The Society of the Plastics Industry, 62–66. The compression set and related properties of flexible urethane foam.

8. L. J. GIBSON and M. F. ASHBY 1988 *Cellular Solids Structure & Properties*. New York: Pergamon Press.
9. N. C. HILYARD 1982 *Mechanics of Cellular Plastics*. New York: Macmillan.
10. J. ICK 1975 *Cellular Plastics in Transportation*, The Society of the Plastics Industry, 16–19. The application of flexible polyurethane foam for automotive seating.
11. H. W. WOLFE 1975 *Cellular Plastics in Transportation*, The Society of the Plastics Industry, 54–61. Factor affecting in HR adduct foam-statistically oriented preparation and evaluation.
12. R. GURRAM and A. VERTIZ 1995 *International Body Engineering Conference and Exposition*. *Detroit*, 1–6. Nonlinear vibration response of automotive seat systems.
13. T. LIBER and H. EPSTEIN 1969 *Shock and Vibration Bulletin* **40**(5), 291–305. Analytic modeling of open-cell forms as shock and vibration elements.
14. K. SHEN, L. LIU, C. MO, M. SUNWOO and W. N. PATTEN 1996 13*th IFAC World Congress*. *San Francisco*, **Q**, 267–272. Predictive feed forward control of an electro-hydraulic automotive seat motion simulator.
15. Z. ZHAO 1995 *M.S. Thesis*, *University of Oklahoma*, *Norman*, *OK*. A measure of automotive seat vibration discomfort.
16. H. DUPIS and G. ZERLETT 1986 *The Effects of Whole Body Vibration*. New York: Springer.
17. E. BERGER and B. J. GILMORE 1993 *Seat Dynamic Parameters for Ride Quality*, SAE paper 930115. Society of Automotive Engineers.

APPENDIX: NOTATION

a, b, c, d_1, p_1, q	coefficients of shape function
A	cushion area
d	foam cell diameter
Δp	pressure difference
E_s	polymer Young's modulus
E_f	foam Young's modulus
ε	strain
$\dot{\varepsilon}$	strain rate
$\boldsymbol{g}$	gravity constant
H	cushion height
K_b	fraction of the total potential open flow area
l	foam cell edge length
M	mass of sandbag
μ	air viscosity
p	fluid, air pressure
ρ	air density
t	foam cell edge thickness
σ	stress
σ_e	elastic stress
σ_f	flow gas effective stress
σ_m	stress of a PUR open cell foam
$\bar{V}$	average velocity
X_0, X_1, X_3	displacement
W_k	kinetic energy loss
W_f	viscous fluid loss
Z_1, Z_2, Z	distance
ζ	volume fraction of open cell matrix